(Preprint) AAS 10-XXX

# OPTIMIZING SPACECRAFT PLACEMENT FOR LIAISON CONSTELLATIONS

C. Channing Chow*, Benjamin F. Villac†, and Martin W. Lo‡

A navigation and communications network is proposed to support an anticipated need for infrastructure in the Earth-Moon system. Periodic orbits will host the constellations while a novel, autonomous navigation strategy will guide the spacecraft along their path strictly based on satellite-to-satellite telemetry. In particular, this paper investigates the second stage of a larger constellation optimization scheme for multi-spacecraft systems. That is, following an initial orbit down-selection process, this analysis provides insights into the ancillary problem of spacecraft placement. Two case studies are presented that consider configurations of up to four spacecraft for a halo orbit and a cycler trajectory.

## INTRODUCTION

The Moon is the closest world to our own and continuing the progression of space exploration will necessitate the understanding of this vital link to the rest of the solar system. With this goal in mind, infrastructure in the Earth-Moon neighborhood is anticipated for both human and cargo transport. We propose to aid in this endeavor with the investigation of potential navigation and communication networks.

Mimicking the function of the GPS system, the proposed concept provides a series of beacons to be used as guideposts for space traffic in the cislunar region. From the standpoint of improving robustness and sustainability, such a constellation should exhibit key features as orbital periodicity and navigation autonomy. These characteristics allow for an effective architecture that will require infrequent stationkeeping maneuvers while minimizing reliance on ground-based tracking for orbit determination support. Note that in simultaneously satisfying both conditions, we enforce a coupling between trajectory design and spacecraft navigation. Fortunately, the framework that provides the most attractive candidates for this pairing is supplied by the natural periodic orbits of the Earth-Moon dynamical system.

Since many classes of periodic orbits are well suited for this type of constellation, a down-selection step is required to reduce the myriad of possible trajectories to a more manageable set (i.e. overcoming local extrema by selecting the best representative from each class to form a smaller, finite subset). This work leverages the dynamical optimization approach presented by Villac et al.[1] to accomplish this first culling step. This paper addresses the second step of the multi-stage constellation design process: the optimization over spacecraft placement.

*Graduate Student; Astronautical Engineering, University of Southern California; channinc@usc.edu
†Assistant Professor; Mechanical and Aerospace Engineering, University of California, Irvine; bvillac@uci.edu
‡Technologist; Jet Propulsion Laboratory, California Institute of Technology; martin.w.lo@jpl.nasa.gov

In this interpretation the optimization metric is obtained from the orbit determination procedure. As seen by a technique developed by Hill, Lo, and Born,[2] autonomous navigation can be achieved between spacecraft orbiting in a multi-body system by exploiting the natural asymmetry of the gravitational field using only satellite-to-satellite telemetry. Hill et al. coined the term LiAISON (Linked Autonomous Interplanetary Satellite Orbit Navigation) to exemplify the method's ability to achieve and maintain a mutual understanding of the satellites' orbital states. Following this convention a spacecraft ensemble utilizing this strategy will be termed a LiAISON constellation.

The present paper begins with a review of the concepts for autonomous navigation followed by the methodology proposed to numerically simulate this optimization problem. Results are presented for two classes of periodic orbits from which one representative trajectory is analyzed for each case: a halo orbit and a cycler trajectory. Finally, the paper concludes with insights gained from this study, followed by an appendix which provides further detail on certain topics discussed in the text.

## AUTONOMOUS NAVIGATION

Typically, spacecraft navigation is achieved via a telemetric connection between the vehicle and the ground segment. Whether that link is between one satellite and a base station or between a constellation and an entire global network, the idea is that the terminals on Earth provide the solution to the orbit determination problem. The notion of autonomy arises when we remove the spacecraft's dependence on terrestrial support and allow them to resolve their states amongst themselves. However, this autonomous navigation concept is not always feasible.

This concept of autonomy is only practical if the results are unambiguous without supplemental input from the ground. That is, the spacecraft states must be uniquely determined solely with the observation set between the spacecraft. Full observability can only be achieved in this manner if the orbits of interest have distinguished shapes within a symmetry class. An orbit is characterized to be unique, or distinguishable, if there does not exist any rotation or translation that will result in another orbit that is also a solution to the original dynamics*. For example, an orbit represented by a state $\mathbf{X}_1(t)$ is said to be distinguishable, if there does not exist a $\theta$ (rotation) and/or $\lambda$ (translation), such that another orbit $\mathbf{X}_2(t)$ can be found to satisfy $\mathbf{X}_2(t) = \theta\mathbf{X}_1(t) + \lambda$. If such a state does exist under these groups of transformations, then the state is no longer observable without additional knowledge. Note that this fact indicates the deterioration of observability in nearly symmetric fields (e.g. small perturbations of a two-body field).

We use the well-known circular restricted three-body problem (CR3BP) as the base model for our time-invariant, conservative system (see Appendix A). The CR3BP provides the simplest dynamical model that captures the actual asymmetry of the Earth-Moon dynamical environment. Here, the appropriate conditions for distinguishable trajectories allow this form of autonomy to be realized. In particular, this study utilizes a novel relative navigation strategy called LiAISON. This technique will be reviewed in the following section along with a description of how we use periodic solutions in the construction of spacecraft constellations cycling between the Earth and the Moon.

*Reflection is omitted from the standard list of global isometries on Euclidean spaces because there exists an unavoidable reflective symmetry about the plane of rotation of the primaries in the chosen system. However, since the ambiguity introduced by this symmetry can be adequately resolved with simple *a-priori* information on the sign of the out-of-plane components, pairs of "North-South" symmetric trajectories are considered locally distinguishable within this symmetry class.

### LiAISON Strategy

Relative autonomous navigation, as introduced by Hill, Lo, and Born,[2] reveals the ability to achieve a mutual understanding of spacecraft orbital states by exploiting the asymmetry of the dynamics. The authors demonstrated indeed that the absolute positions of a pair of spacecraft can be retrieved from observing the relative positions of the satellites along periodic orbits in the CR3BP. As long as one spacecraft maintains a distinguishable trajectory, then both states can be fully characterized with the knowledge of their observations alone.[3]

By employing a weighted batch filter in a statistical orbit determination approach (see Appendix B), a best estimate of the spacecraft states is found using only satellite-to-satellite range measurements as the input data type. This reduction to mere scalar measurements of range allows for a simpler modeling of the errors associated with the navigation process. From the linearized measurement model about a reference trajectory

$$\mathbf{y}_i = \tilde{H}_i \hat{\mathbf{x}}_i + \hat{\boldsymbol{\epsilon}}_i \qquad \text{for } i = 1 \dots \ell \tag{1}$$

for $\ell$ observations, where $\tilde{H}_i \hat{\mathbf{x}}_i$ is a mapping of the estimated initial state deviation to the observation space, $\hat{\boldsymbol{\epsilon}}_i$ is the unknown observation error and $\mathbf{y}_i$ is the observation residual that encompasses the range measurements. If the errors are modeled well, in a least-squares sense, the convergence criteria becomes easier to compute when handling only one data type. The weighted root-mean square of the estimated errors of Eq. (1) is defined as

$$\text{WRMS} = \left[ \frac{1}{m} \sum_{i=1}^{\ell} \hat{\boldsymbol{\epsilon}}_i^T R_i^{-1} \hat{\boldsymbol{\epsilon}}_i \right]^{1/2} \tag{2}$$

where $R_i$ is the covariance of the data noise and $W_i$ is the weighting matrix that can be computed from $W_i = R_i^{-1}$, with diagonal entries $[W_{pp}] = 1/\sigma_p^2$ for $p-$dimensional data types ($\sigma$ are the standard deviations of the data noise). In our case where $p = 1$, the total dimension of $\hat{\boldsymbol{\epsilon}}$ is $\ell \times 1$ (since $m = p \times \ell$), reducing Eq. (2) to WRMS $= \sqrt{(\hat{\boldsymbol{\epsilon}} \cdot \hat{\boldsymbol{\epsilon}}) \,/\, (\ell \sigma^2)}$. This simplification is particularly useful in this study for processing orbits with large periods, and hence, many observations.

### Periodic Constellations

Regions that span large variations in acceleration prove to yield the best LiAISON performance. Among the most attractive candidates for this type of navigation are trajectories that are strongly influenced by both primaries. Inasmuch as one constraint for the LiAISON strategy imposes maintaining distinguishable orbits, these trajectories should also be ideally suited for constellation design in terms of coverage. In other words, not all distinguished orbits will prove useful for cislunar infrastructure.

One of the advantages of using the CR3BP is the availability of such trajectories: the set of periodic* orbits affords distinguishable solutions that are well primed to support spacecraft constellations. While the notion of a constellation is not restricted to periodic motion, it is associated with bounded variations in time of the relative configurations between two or more spacecraft. Placing a sequence of spacecraft on a single periodic orbit offers the simplest possible constellation with

*These periodic orbits are quasi-periodic in higher fidelity models of the same dynamical system.

periodic variations in time. Since this restricted class of constellations is still large, another scheme is required to reduce the set.

The systematic procedure of reducing different families of periodic orbits to only a few prospective members is a variational problem that has been addressed in the dynamic optimization step.[1] It is only after this first stage of down-selection that this study is applicable. For the present case, two classes of orbits that have been shown to exhibit desirable properties for constellation design are considered: a halo[4] orbit and a cycler[5] trajectory.

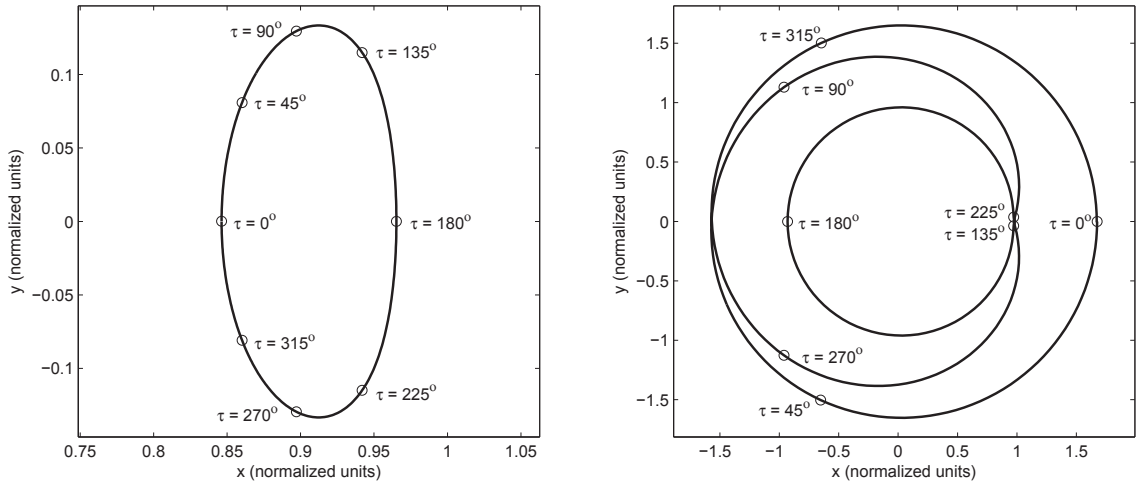


**Figure 1. Positions of various phase angles on planar projections of two periodic orbits in the Earth-Moon system. (Left) Halo orbit. (Right) Cycler trajectory.**

The vicinity of the equilibrium points and regions that roam the periphery of both primaries do indeed present some interesting options for this study. Halo orbits near the libration points have short periods and provide localized coverage of the lunar surface, whereas cycler orbits have much larger periods and can support transportation within the Earth-Moon system. Figure 1 illustrates a representative of each of these types of orbits, specifically highlighting how the phasing of spacecraft would be affected by different orbital geometries (note the multiple flybys of the Moon experienced by the cycler trajectory around $135°$ and $225°$). Given an orbital period $T$, the phase angle is defined as:

$$\tau = \frac{2\pi}{T}\Delta t \tag{3}$$

After the initial culling process, from which these candidates are identified, further optimization is required to select the appropriate number of spacecraft and properly phase them around the orbit. This optimization step is the subject of the present paper.

## NUMERICAL ANALYSIS

The focus of this work is to understand the impact of spacecraft placement on LiAISON constellation design. We numerically simulate various constellation geometries such that every relative combination* of spacecraft placements is explored and then optimize over this set. Optimal, in this

*An approximation to a continuous set is made by taking discrete intervals in phase shifts.

sense, refers to the configuration of spacecraft that will achieve the best autonomous navigation performance when using the LiAISON technique. In particular, we are searching for the formation that will minimize the navigation errors as captured by the $\beta_{\text{ave}}$ metric[3] (see Eq. (6)).

Globally, this problem is a finite-dimensional optimization problem over several real variables, namely the set of relative phases $\tau_i$, parameterized by the number of spacecraft. That is, the problem is handled as separate local optimizations over time shifts for each configuration. This organization alleviates the computational intensity required to solve the whole problem at once, especially since each local run uses an exhaustive search approach to survey the solution space. This exhaustive methodology is proposed to help understand the structure of local extrema, and in effect, to better characterize the more general optimization problem for use with other numerical routines. The details of this method and associated terminology are described next.

Note that the time-invariant nature of the dynamics implies that a constellation of $N$ spacecraft is determined by $N-1$ phases. It is therefore only convenient to graphically represent the solution for up to $N = 4$. In fact, this study investigated constellations of up to four spacecraft for one halo orbit and one cycler trajectory. The optimization results are given separately in the following sections.

**Optimization Over Time Shifts**

The spacecraft placement problem is tackled as a parameterized optimization problem over the relative time shifts (or phases) between the satellites. Recall that the phase angle defined in Eq. (3) is a non-geometric angle. This phasing can be considered a shift in time normalized by one orbital period. The result is analogous to mean anomaly in two-body dynamics, in that $\tau$ has a constant time derivative.

Let the initial state of the $i^{\text{th}}$ spacecraft be $\mathbf{X}_i(t_0)$. Its state at any other point on the orbit can be expressed as $\mathbf{X}_i(t) = \phi\left(t, t_0, \mathbf{X}_i(t_0)\right)$, where the function $\phi$ denotes the flow* (solution) of the dynamics. Since any spacecraft in the sequence can theoretically be measured from the position of any other spacecraft, the state of the $j^{\text{th}}$ spacecraft at time $t$ can be written as

$$\mathbf{X}_j(t) = \phi\left(\Delta t_{ij}, t, \mathbf{X}_i(t)\right) \qquad \text{for } i, j = 1, 2, \ldots, N\,, \quad i \neq j \tag{4}$$

where $\Delta t_{ij}$ represents the time shift, or equivalently, the phase separation $\tau_{ij}$ between the $i^{\text{th}}$ and $j^{\text{th}}$ spacecraft. This convention allows the consideration of only the relative positions between any pair of satellites along the chosen periodic orbit. The number of combinations of pairs increases via the "n-choose-k" function from combinatorics and is therefore non-linear with respect to the number of spacecraft ($N$). Although implicitly not a limitation of the original problem, a restriction is imposed to consider only spacecraft relative to their immediate neighbors (i.e. reducing the number of pairs to $N$). This constraint simplifies the notation from $\tau_{ij}$ to $\tau_i$, effectively removing the explicit indexing over the $j^{\text{th}}$ spacecraft, since only consecutive pairs are now considered. For example, $\tau_k$ will denote the phase angle between spacecraft $k$ and $k+1$. An absolute configuration can thus be obtained by defining the placement of just one spacecraft, say the first. The state of any spacecraft relative to the previous one is now defined as

$$\mathbf{X}_{i+1}(t) = \phi\left(t_i, t, \mathbf{X}_i(t)\right) \qquad \text{for } i = \text{mod}\left(1, 2, \ldots, N;\ N\right) \tag{5}$$

*From the theory of ordinary differential equations, the mathematical model of a deterministic process is called a phase flow.[6] That is, the flow represents the integration of the dynamics over time.[7]

The performance metric used for this optimization step originates from a weighted batch least-squares filter. The $\beta$ parameter is defined as $3\sigma$ of the largest error of the orbit determination solution (see Appendix B). Several iterations on this definition are required to obtain a metric more relevant to a constellation. Since $\beta$ results from the analysis of a pair of spacecraft at each increment in time, $\bar{\beta}$ may be computed as the average over the fit span. Furthermore, for constellations where multiple pairs are possible, $\bar{\beta}$ can be averaged over the number of pairs considered producing $\beta_{\text{ave}}$.

$$\bar{\beta} = \frac{1}{n}\sum_{i=1}^{n}\beta_i \qquad ; \qquad \beta_{\text{ave}} = \frac{1}{N}\sum_{j=1}^{N}\bar{\beta}_j \tag{6}$$

for $n$ increments in the fit span and $N$ pairs. Recall, because the number of pairwise combinations of $N$ spacecraft is constrained to consecutive pairs, the number of pairs is implied. Although we treat constellations of up to only four spacecraft, the general $N$ spacecraft optimization problem is formulated as

$$\min_{\tau_1,\ldots\tau_N}\left(\beta_{\text{ave}}(\tau_1,\ldots,\tau_N)\right) \tag{7}$$

**Modeling and Simulation**

Given the initial conditions obtained from the down-selection process, a baseline orbit is established by integrating the trajectory forward for one full period. Figure 2 illustrates the scale of the halo orbit as compared to the cycler trajectory. To populate the constellation, we punctuate the orbit with $N$ satellites at varying degrees of separation. The first spacecraft is placed on the $x-$axis (i.e. line of symmetry), thereby defining $0^\circ$ in $\tau-$space. Note that, due to the time-invariance of the dynamics, a spacecraft placed anywhere on the orbit will yield the same navigation accuracy as long as the fitting interval is an integer multiple* of one orbital period. As such the configuration that offers the simplest routine is preferred. Every subsequent phase shift is taken in increments of $\Delta\tau = 15^\circ$ (implicitly constraining the minimum separation between neighboring spacecraft as well). Sequential loops are then constructed to perform an exhaustive search on each combination of spacecraft taken two at a time.

Spacecraft are propagated forward for the desired length of time (either for $T/2$ or $T$) and measurements are made at preset increments. This propagation length defines the fit span. In this study occultations are not modeled and so the simulated range measurements are uninterrupted. Depending on the size of the periodic orbit, different sampling frequencies are used to maintain a reasonable amount of observations taken throughout the fit span. Note that too few observations will lead to an unobservable state. Generally, a frequency of either 0.001 or 0.0001 time units (about 375 or 37.5 seconds, respectively) is used with white noise added at a standard deviation of 1 m. A perturbation of 1 km and 1 mm/s (in position and velocity, respectively) is given to the known initial conditions to emulate an initial guess for the filter.

Once the data is generated, a weighted batch least-squares filter is applied to estimate the initial states for each pair of spacecraft. This method involves supplying the initial state estimate along with a series of observations that is then iteratively refined until a best estimate is converged upon. This process is referred to as statistical orbit determination and is analogous to curve fitting. One of the key features of this algorithm is the ability to accept measurements at different times during a fitting interval. Through the aid of the state transition matrix, a measurement at any time $t_i$ may

*Assuming an exact periodic orbit, for any integer $k$, $\mathbf{X}(t) = \mathbf{X}(t + kT)$.

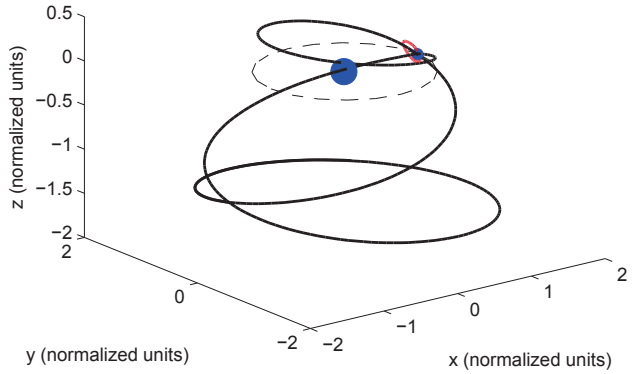


**Figure 2. A halo orbit (red) and a cycler trajectory (black) as seen from the rotating frame. The Earth and Moon are shown as the larger and smaller dots (blue), respectively. A unit circle (dashed line) is included for scale.**

be related back to a desired epoch $t_k$ by applying $\hat{\mathbf{x}}_i = \Phi(t_i, t_k)\hat{\mathbf{x}}_k$ to Eq. (1). Moreover, because of the linearization of the dynamics and measurement model about a reference trajectory, each observation is treated individually as a separate equation. Thus, ephemeris files may be constructed to an arbitrary length (at least greater than the number of state variables). Accumulating the measurements from a set of ephemeris data into one matrix equation lends the notion of this scheme as being a "batch" processor.

The success of the LiAISON strategy depends on the spacecraft states being fully observable. That is, the state variables must be linearly independent. To ensure that this occurs in a numerical routine is to validate that the information matrix is full rank and has a condition number less than $10^{16}$ (which also helps with matrix inversion). Additionally, during the curve fitting process the convergence criteria as given in Eq. (2) is iterated over until a steady state is reached, namely when the rate of change of the WRMS falls below $10^{-9}$. The stability of this process greatly affects the convergence rate of the entire simulation.

Accuracies of the filter, and hence representations for navigation performance, are computed in $\beta_{\text{ave}}$ as given in Eq. (6). And as part of the exhaustive search, each combination of spacecraft pairing will yield a different error metric. The set of $\beta_{\text{ave}}$ is evaluated and plots are generated to graphically represent the solution space. These figures are provided in the following section along with specific parameters associated with particular runs.

## OPTIMIZATION RESULTS FOR SPACECRAFT PLACEMENT

### Halo Class

*Halo - 2 Spacecraft.* Figure 3 illustrates the navigation accuracy of the batch filter as obtained for two spacecraft on a single halo orbit with a continuous observation arc of one orbital period.

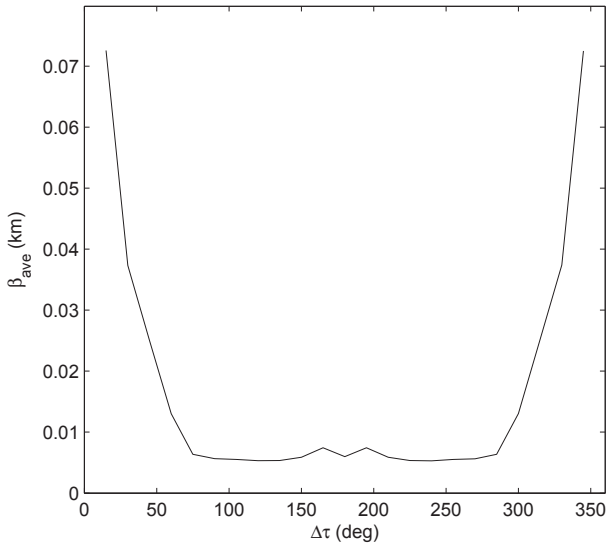


**Figure 3. Navigation accuracy as achieved by a two-spacecraft halo constellation at varying combinations of phase separation.**

A similar trend in performance was recovered, as observed by Hill et al.[3] This structure likewise indicates better estimation errors above/below $\pm 75^{\circ}$, respectively. This result supports a LiAISON design guideline that suggests placing spacecraft at large separation distances (rather than in closer formations) improves navigation performance.

Ostensibly, this plot infers an indifference to the direction of the change in phase between the pair of satellites. Note, however, that this apparent symmetry is only an artifact of placing the first spacecraft on the line of symmetry of the halo orbit and using a fitting interval of exactly one orbital period.

Trials were conducted using varying fitting intervals ranging from $T/2$ to $T$. Aside from destroying the symmetry of the estimation accuracies, the solution actually became unobservable as the fit span approached the limit of half an orbital period. It is guessed that the length of the observation arc must contain a section that traverses the orbital line of symmetry in order to properly converge. Since this work enforced the convention of placing the leading spacecraft on the line of symmetry, future investigations into off-axis starting points are required to better characterize this limitation.

Returning to the current symmetry observed in the figure, two symmetric global minimums indeed occur at $\pm 120^{\circ}$ along with a local minimum located at $180^{\circ}$. Some extrema correspond well with salient geometric features of the halo orbit itself, such as the extremities of the $z-$amplitude, while others only come near features like the $(x, y)-$plane crossings. The explicit geometric link between the trajectory profile and navigation performance is still not fully understood. Nonetheless, the orbit determination process exhibits a clear preference towards larger spacecraft separations when applying the LiAISON strategy.

*Halo - 3 Spacecraft.* Continuing the parameterization sequence for three spacecraft, Figure 4 depicts the angle space generated by the first and second spacecraft, with the $\beta_{\text{ave}}$ parameter shown in the color dimension. Here, the truncation of the solution space to a lower triangular grid is the

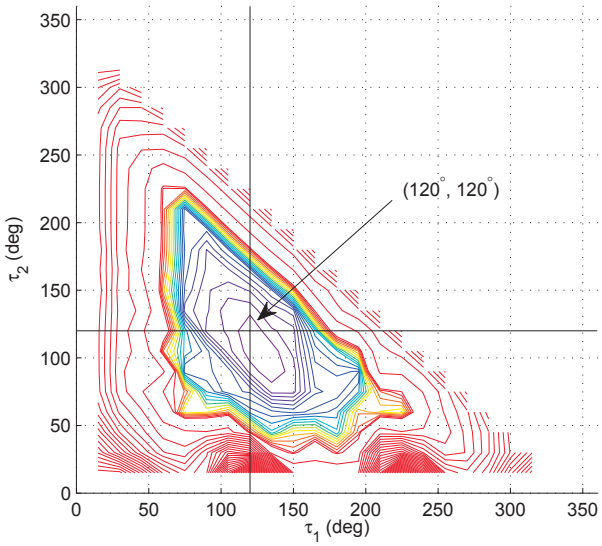


**Figure 4. Navigation accuracy as achieved by a three-spacecraft halo constellation over all phase combinations, where $\beta_{\text{ave}}$ is presented in the color dimension, ranging from about 5m to 100m. The global minimum is indicated at $(120°, 120°)$.**

result of preserving the spacecraft ordering. That is, since the sum of all phase shifts is necessarily $360°$, the $N^{\text{th}}$ spacecraft phasing is inferred from the sum of the others, thus limiting the possible combinations allowed in the solution space. Note, the coarse $15°$ sampling increment creates the step-like feature of the hypotenuse.

The empty margin bordering the axes is due to enforcing the constraint of a $15°$ minimum spacecraft separation. However, if a pair of satellites were allowed to approach a zero phase angle (i.e. a collocation condition), the group would deform to an $N-1$ constellation. Although an identical collocation condition could be reached by reducing any phase angle to zero, this tendency is actually path dependent. For example, as the spacecraft separations tend towards zero in $\tau_1$ and $\tau_2$, possible configurations could be $(1°, 15°, 344°)$ and $(15°, 1°, 344°)$ respectively. These arrangements are clearly different and indeed do contribute to dissimilar structures that are most pronounced near the fringes. More surprisingly though, a global extrema is seen to develop roughly concentrically around the coordinates $(120°, 120°)$. This minimum identifies the points of an equilateral triangle formation in angle space, giving the first indication that evenly spaced spacecraft may yield the optimal configuration.

*Halo - 4 Spacecraft.* Because the solution space generated by the set of three phase angles is volumetric, Figure 5 previews the interior of the volume via slice planes at varying increments that are parallel to each face of the volume. Again, with $\beta_{\text{ave}}$ represented in the color dimension, the formation of a minimum develops towards the center of the volume. In fact, the global minimum is reached at $(90°, 90°, 90°)$. Even as the number of spacecraft is increased, the optimal scenario is still one where the spacecraft are evenly spaced around the orbit. This observation further reinforces the notion of a regular polygon arrangement as mapped onto an orbit.

Moreover, we conjecture that the optimal configuration for an $N$ spacecraft constellation is a corresponding regular $N-$gon in terms of equal relative phase. However, to bound the conclusion,

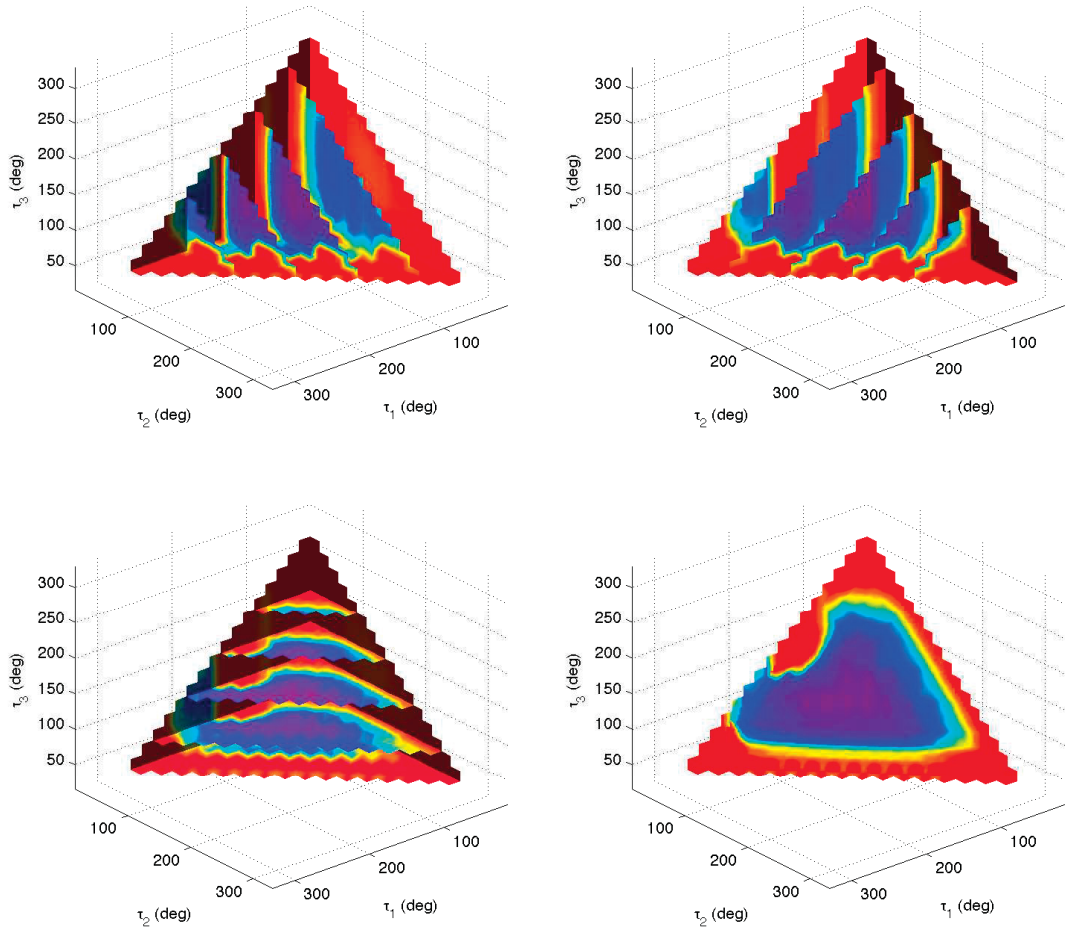


**Figure 5. Navigation accuracy as achieved by a four-spacecraft halo constellation over all phase combinations, where $\beta_{\text{ave}}$ is presented in the color dimension, ranging from about 17m to 385m. The volumetric data is previewed by four plots featuring slice planes parallel to each face of the volume.**

we must only claim our conjecture to hold for orbits that share similar characteristics with the present halo orbit.

To clarify, though an optimal configuration can theoretically be reached for any given number of spacecraft, the navigation performance does not necessarily improve with the addition of more spacecraft. For instance, the $\beta_{\text{ave}}$ value for the four spacecraft case reached a slightly poorer accuracy of around 17m as compared to both the two and three spacecraft cases with accuracies of around 5m. This slight decrease in estimation accuracy is expected since the regular $4-$gon configuration has phase angles that are less than the optimal spacing identified for a pair of satellites (as discovered in the two spacecraft case to be $120^\circ$). Note that the decline in navigation performance is only noticeable beyond the three spacecraft configuration where the phase separations were precisely at the optimal spacing. This observation actually identifies the critical limit on the number of spacecraft for this halo constellation, in terms of navigation accuracy, to be three spacecraft.

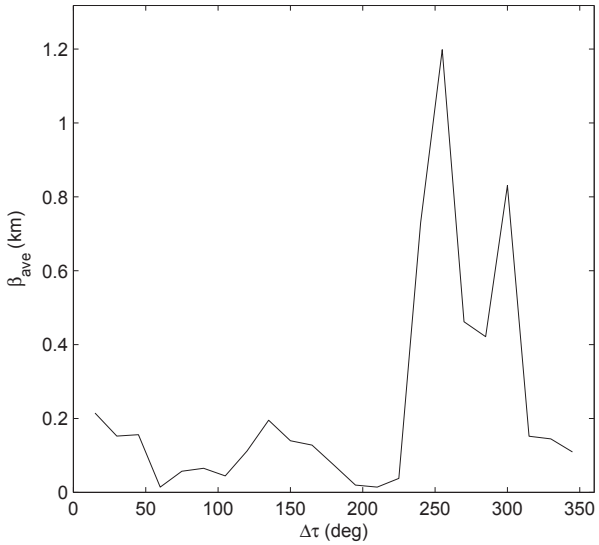


**Figure 6. Navigation accuracy as achieved by a two-spacecraft cycler constellation at varying combinations of phase separation.**

*Cycler - 2 Spacecraft.* The cycler trajectory presents results far less intuitive as compared to those of the halo orbit. Several trial analyses were performed to determine the appropriate fitting interval, again ranging from $T/2$ to $T$. This time the observation was the opposite, namely the batch filter improved as the fit span approached half an orbit and in fact failed entirely for a fit span of one full period. For a fitting interval of a non-integer multiple of an orbital period, one can no longer take advantage of the time-invariance of the dynamics and must concede to choosing a starting point, acknowledging that a different choice will produce different results. Recall, the choice for the starting location of the lead spacecraft is on the $x-$axis.

Figure 6 shows how the estimation errors vary as the spacecraft formation move from apogee towards both periselene flybys during their $180^\circ$ measurement window. The presence of several jagged local extrema make it difficult to draw insightful conclusions from this data. However, the sharp transition from a local minimum to a local maximum around $225^\circ$ does indeed suggest some underlying structure. When compared to the phase portrait of the cycler orbit (Figure 1, right side), it is evident that a spacecraft starting at that location will not experience either of the lunar flybys. Conversely, the first instance where a spacecraft would encounter both flybys is around $60^\circ$, which corresponds nicely with an observed local minima of roughly $14$m accuracy. This observation marks a poignant implication that close flybys may play an important role in the observability of spacecraft states.

*Cycler - 3 Spacecraft.* Adding a third spacecraft to the constellation indeed helped pronounce the more prominent structures in the phase space. Two striking features of Figure 7 are the diagonal band centered on the line $\tau_1 = 250^\circ - \tau_2$ and the valley centered on the line $\tau_1 = 60^\circ$. The $100^\circ$ width diagonal band corresponds to the bottom half of the cycler orbit that sits almost entirely below the plane of rotation of the primaries (see Figure 2). Since in an inertial sense, this observation arc is mainly in the apogee half of an elliptic orbit, the conditions of inconjugacy are not well

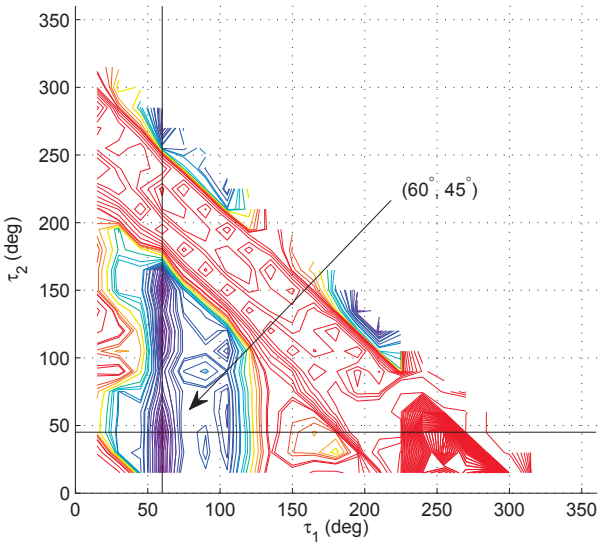


**Figure 7. Navigation accuracy as achieved by a three-spacecraft cycler constellation over all phase combinations, where $\beta_{ave}$ is presented in the color dimension, ranging from about 35m to 110km. The global minimum is indicated at $(60°, 45°)$.**

realized. That is, given measurements taken during this fitting interval, the filter could easily confuse this portion of an orbit as belonging to a number of valid elliptic orbits. Hence, poor navigation performance within this region is expected and, in fact, is shown to reach errors in excess of 100km.

Naturally, the navigation results are anticipated to improve as the fitting interval gradually moves towards the regions of high asymmetry near the Moon and the measurements start to incorporate observations during the first flyby. Indeed, some minor improvement is seen, however irregular. This mediocre response is due to the fact that only one flyby was covered. Since the flybys exhibit very sensitive scattering effects associated with close approaches to the gravity well, the rigidity given to an orbit through one flyby is minimal and laced with uncertainty. On the other hand, if two or more flybys are encountered then a much better sense of the orbit can be obtained.

The centerpiece of this data is really the valley of local minimums that appear around $\tau_1 = 60°$. Here the global minimum is of less interest than the trend expressed by the local minimums. Recall that $\tau_1 = 60°$ corresponds to the first (but not only) instance where the second spacecraft would encounter both flybys during the fit span. Whereas the emphasis on "first" is somewhat arbitrary, a more important distinction should be made that this occurrence also corresponds to the most asymmetric arc out of the family of arcs that span both flybys. This asymmetry coupled with the rigidity offered from the multiple flybys helps the filter accurately converge on a distinguishable orbit. Surprisingly, though the conclusion could be drawn that all spacecraft should experience multiple flybys, this valley structure indicates a weak dependence on $\tau_2$, implying that actually the observability is conditioned by requiring only one spacecraft to maintain a distinguishable trajectory.

Unfortunately, numerical difficulties with the convergence for the four spacecraft cycler constellation prevented the completion of the gamut of simulations. Several resolution avenues are under investigation. Additionally, because of the limitation of computation power (and time) the cycler cases were run with reduced convergence tolerances making direct one-to-one comparisons with the

halo results difficult to draw. Since a full simulation ranges from days to weeks to complete, each run consumes a non-trivial amount of wallclock time. This work is part of an on-going effort.

## CONCLUSIONS

In this paper we studied the ancillary spacecraft placement problem for several Earth-Moon navigation and communication networks. In particular, we proposed to utilize the autonomous navigation technique of the LiAISON strategy as applied to a series of spacecraft placed on periodic orbits, called LiAISON constellations. A finite dimensional optimization problem was formulated over the span of phase shifts between pairs of spacecraft on these constellations. Parameterizing by the number of satellites allowed for separate, smaller local optimization problems to be analyzed. The optimization metric was derived from a statistical orbit determination procedure and was specifically chosen to be an indicator of navigation performance: the $\beta_{\text{ave}}$ parameter.

To demonstrate this analysis, two case studies were presented. Simulations were conducted for a halo orbit and a cycler trajectory. Since this spacecraft placement problem ideally follows an initial orbit down-selection process, both of these orbits were assumed to have optimized some local continuation parameter during the first step. Several $N-$constellations for each orbit were analyzed, namely, the cases for two and three spacecraft ensemble for both the halo and the cycler plus an additional four spacecraft configuration for the halo orbit, yielding a total of five simulations.

The results from the halo analysis showed that a regular $N-$gon arrangement of spacecraft, as mapped onto a halo orbit, provided the optimal configuration for autonomous navigation. This outcome reinforced the intuitive notion that evenly placed spacecraft along an orbit will constitute the best scenario. However, a limitation is noted. It is seen that the navigation performance deteriorated as the spacecraft separation approached zero, suggesting that close formation flying would actually yield poorer state estimations. In fact, beyond the nominal spacing of $120^\circ$ between spacecraft, the navigation performance experienced declines in accuracy, thus suggesting the critical limit for this halo constellation to be three satellites in an equilateral triangle formation.

Interestingly, the cycler analysis revealed different insights into the structure of the spacecraft placement problem that were not present in the halo class. Covering a fundamentally larger gravitational regime, the cycler orbits spent considerable time away from the vicinity of the smaller primary (Moon) and hence were often dominated by the two-body dynamics of the larger primary (Earth). In this particular case, the cycler trajectory had two close flybys of the Moon, thus encountering regions of high asymmetry in the gravitational field; a necessity for the LiAISON method. Indeed, the simulations indicated the configuration that achieved the lowest estimation error was the case where at least one of the satellites experienced both flybys during an asymmetric measurement interval. Though one flyby provided a more rigid orbit, the second flyby solidified this rigidity by removing the uncertainty caused by the sensitive scattering effects associated with the close approach to the Moon. Ultimately, this stabilization isolated the distinguished orbit, thereby making the states fully observable. In this close flyby environment, the even spacing notion is supplanted by a more physics-driven phasing arrangement: namely one that favors multiple flybys over an asymmetric observation arc.

## ACKNOWLEDGMENT

This work has been supported in part by the Steckler Space Grant Space Colonization Program managed by the California Space Grant Consortium. We are thankful to Mike Wiskerchen of Space

Grant for this support. This work has been supported in part by the EPISODE Project of the NASA Advanced Information Science Research Program. This work was performed in part at the Jet Propulsion Laboratory, California Institute of Technology under a contract with the National Aeronautics and Space Administration.

## APPENDIX A: CIRCULAR RESTRICTED THREE-BODY PROBLEM

The circular restricted three-body problem (CR3BP) approximates the dynamics of a particle of negligible mass $m$ moving in a system under only the gravitational influence of two finite bodies of mass $m_1$ and $m_2$ (where $m_1 \geq m_2$ and both are assumed to be point masses). The motion of the primaries defines the $(x, y)-$plane, where the two bodies mutually orbit their center of mass or barycenter. This implies a normally directed $z-$axis that is parallel to the angular momentum vector of the rotating system. Additionally, the synodic coordinate system is typically chosen such that the $x-$axis is aligned to and rotates with the syzygy (Earth-Moon) axis, allowing the primaries to appear stationary. For convenience, non-dimensional parameters are chosen to normalize key

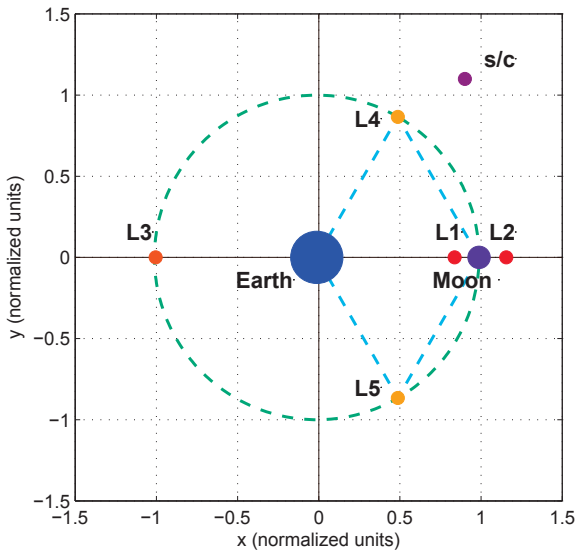


**Figure 8. Schematic representation of the normalized CR3BP synodic coordinate system with libration points for $\mu \simeq 0.01215$.**

quantities related to the primaries. More specifically, the following are all set to unity: the sum of the two masses, the mean distance between their centers, their mean motion about the barycenter, and the gravitational constant. Furthermore, a mass ratio[7] is defined as: $\mu = m_2/(m_1 + m_2)$. Using this normalized convention, the masses are described as, $m_1 = (1 - \mu)$ and $m_2 = \mu$. With a unit angular velocity, the orbital period of the primaries is necessarily equal to $2\pi$. At a unit separation distance, the locations of the Earth and Moon respectively are $x = -\mu$ and $x = (1 - \mu)$, as shown in Figure 8. This figure also indicates the location of the five relative equilibrium points, or lunar libration points L1, . . ., L5, for a system with $\mu \simeq 0.01215$.

The equations of motion in the non-dimensionalized CR3BP are:

$$\ddot{x} = 2\dot{y} - \frac{\partial \overline{U}}{\partial x} \quad ; \quad \ddot{y} = -2\dot{x} - \frac{\partial \overline{U}}{\partial y} \quad ; \quad \ddot{z} = -\frac{\partial \overline{U}}{\partial z} \tag{A1}$$

where the effective potential $\overline{U}$ is given as: $\overline{U} = -\frac{1}{2}\left(x^2+y^2\right) - \frac{(1-\mu)}{r_1} - \frac{\mu}{r_2}$, and the spacecraft distances with respect to the Earth and Moon are denoted respectively, $r_1 = \sqrt{(x+\mu)^2+y^2+z^2}$ and $r_2 = \sqrt{(x-1+\mu)^2+y^2+z^2}$.

## APPENDIX B: STATISTICAL ORBIT DETERMINATION

Orbit determination simulations were performed using a batch processor following the design presented in Tapley, et al.[8] Crosslink range measurements were generated with normally distributed Gaussian noise to estimate the 12-state vector (two concatenated 6-state vectors for a pair of spacecraft)

$$\mathbf{X} = \begin{bmatrix} x_1 & y_1 & z_1 & \dot{x}_1 & \dot{y}_1 & \dot{z}_1 & x_2 & y_2 & z_2 & \dot{x}_2 & \dot{y}_2 & \dot{z}_2 \end{bmatrix}^T \tag{B1}$$

By minimizing the performance index that accommodates *a priori* values, the method of weighted least-squares is applied to solve the normal equations

$$\Lambda \hat{\mathbf{x}}_0 = N \tag{B2}$$

where the solution $\hat{\mathbf{x}}_0$ is the best estimate of the initial state deviation vector. The information matrix, $\Lambda$, and the state residuals vector, $N$, are accumulated per observation as

$$\Lambda = \overline{P}_0^{-1} + \sum_{i=1}^{\ell} H_i^T W_i H_i \qquad ; \qquad N = \overline{P}_0^{-1}\overline{\mathbf{x}}_0 + \sum_{i=1}^{\ell} H_i^T W_i \mathbf{y}_i \tag{B3}$$

for $\ell$ observations. $\overline{P}_0$ is the *a-priori* covariance matrix, $H$ is the observation-state mapping matrix, $W$ is the weighting matrix, $\overline{\mathbf{x}}_0$ is the *a-priori* estimated state deviation vector, and $\mathbf{y}$ is the observation residuals vector. Note the performance index is

$$J(\hat{\mathbf{x}}_0) = \frac{1}{2}\left(\hat{\mathbf{x}}_0 - \overline{\mathbf{x}}_0\right)^T \overline{P}_0^{-1}\left(\hat{\mathbf{x}}_0 - \overline{\mathbf{x}}_0\right) + \frac{1}{2}\sum_{i=1}^{\ell}\left(\mathbf{y}_i - H_i\hat{\mathbf{x}}_0\right)^T W_i \left(\mathbf{y}_i - H_i\hat{\mathbf{x}}_0\right) \tag{B4}$$

The inverse of the information matrix yields the initial covariance matrix, $P_0 = \Lambda^{-1}$. Propagated over the fit span using, $P_i = \Phi\left(t_i, t_0\right) P_0 \Phi^T\left(t_i, t_0\right)$, the batch covariance matrix provides the error distribution at each time $t_i$. From the eigendecomposition of the covariance matrix, $P = QDQ^{-1}$, the $\beta$ parameter is defined at any epoch to be

$$\beta = 3 \max\left(\sqrt{[D_{jj}]}\right) \qquad \text{for } j = 1, 2, 3 \tag{B5}$$

## REFERENCES


[1] B. Villac, C. Chow, M. Lo, and G. Hintz, "Dynamic Optimization of Multi-Spacecraft Relative Navigation Configurations in the Earth-Moon System," *Journal of Astronautical Sciences (pre-print)*, 2010.

[2] K. Hill, M. Lo, and G. Born, "Linked, Autonomous, Interplanetary Satellite Orbit Navigation (LiAISON)," *Advances in the Astronautical Sciences*, Vol. 123, Part III, 2006, pp. 2353–2367.

[3] K. Hill and G. Born, "Autonomous Interplanetary Orbit Determination Using Satellite-to-Satellite Tracking," *Journal of Guidance, Control, and Dynamics*, Vol. 30, No. 3, 2007, pp. 679–686.

[4] K. Howell, "Three-Dimensional, Periodic, Halo Orbits," *Celestial Mechanics*, Vol. 32, 1984, pp. 53–71.

[5] J. Casoliva, J. Mondelo, B. Villac, K. Mease, E. Barrabes, and M. Olle, "Two Classes of Cycler Trajectories in the Earth-Moon System," *Journal of Guidance, Control, and Dynamics*, Vol. 33, No. 5, 2010, pp. 1623–1640.

[6] V. Arnold, *Ordinary Differential Equations*. Cambridge, MA: The MIT Press, 1973.

[7] V. Szebehely, *Theory of Orbits*. New York, NY: Academic Press, Inc., 1967.

[8] B. Tapley, B. Schutz, and G. Born, *Statistical Orbit Determination*. Burlington, MA: Elsevier Inc., 2004.